Journal of
Synchrotron Radiation

ISSN 0909-0495

Received 6 March 2012
Accepted 25 March 2012

On easily tunable wide-bandpass X-ray monochromators based on refraction in arrays of prisms

Werner Jark

Sincotrone Trieste ScpA, SS 14 km 163.5, I-34012 Basovizza (TS), Italy.
E-mail: werner.jark@elettra.trieste.it

Refractive lenses focus X-rays chromatically owing to a significant variation of the refractive index of the lens material with photon energy. Then, in combination with an exit slit in the focal plane, such lenses can be used as monochromators. The spectral resolution obtainable with refractive lenses based on prism arrays was recently systematically investigated experimentally. This contribution will show that a wide-bandpass performance can be predicted with a rather simple analytical approach. Based on the good agreement with the experimental data, one can then more rapidly and systematically optimize the lens structure for a given application. This contribution will then discuss more flexible solutions for the monochromator operation. It will be shown that a new monochromator scheme could easily provide tuning in a fixed-exit slit.

Keywords: X-ray refraction; focusing; monochromator; fixed-exit slit; wide bandpass.

1. Introduction

The use of different forms of arrays of prisms as X-ray monochromators has already been discussed (Cederstrom, 2001; Jark, 2004; Fredenberg *et al.*, 2008, 2009). These objects focus in only one dimension. The bi-dimensionally focusing case with stacks of concave circularly symmetric lenses has also been reported (Vaughan *et al.*, 2011). Recently, Liu *et al.* (2012) presented systematic experimental data for obtaining spectral resolution at synchrotron radiation sources using refractive lenses of the prism array or clessidra type (Jark *et al.*, 2004*b*, 2008). In this type of lens the number of small identical X-ray refracting prisms increases linearly with distance from the optical axis, as shown in Fig. 1. This concept was introduced in order to minimize the intensity losses owing to absorption (Jark *et al.*, 2004*b*). As these lenses are not yet integrated into ray-tracing programs, Liu *et al.* (2012) simulate the tendencies in the expected performance by ray-tracing symmetric cylindrical lenses with concave surfaces for one-dimensional focusing. Here it will be shown that the performance of these prism arrays for monochromatization purposes can be predicted analytically. This will make the optimization a much faster and more precise task. First studies indicate more favourable and flexible operation schemes compared with the reported case. Finally, a new scheme for a tunable wide-bandpass X-ray monochromator with fixed exit slit is presented.

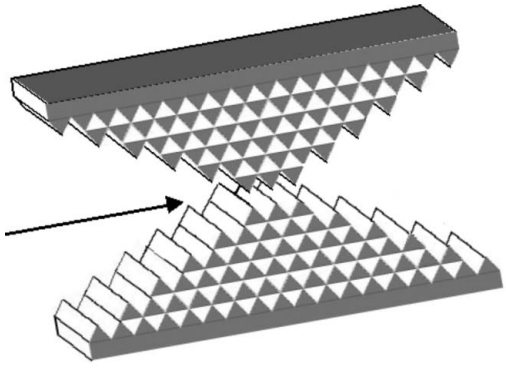

Figure 1
Scheme of an axially symmetric clessidra lens which focuses one-dimensionally. In the presented structure the number of small identical prisms is increasing by three between adjacent rows.

2. Theoretical considerations

Lengeler *et al.* (1999) introduced the concept of the effective aperture $A_{\rm eff}$ for the calculation of the transmission through absorbing structures. This aperture is the transmission function of the structure integrated over its geometrical aperture $A_{\rm geo}$, *i.e.* either over its diameter or over an upstream smaller beam-limiting aperture. The effective aperture allows us thus to calculate the photon flux to be found behind the structure.

The prism array structure clessidra for the focusing of X-rays is characterized by the following parameters: j = row index, $J_{\rm max}$ = index of last row, M = prism number increment between rows, φ = angle of incidence of the rays onto the prism side walls, h = prism height, AL = attenuation length of the prism material. The lens in Fig. 1 has $J_{\rm max} = 6$, $M = 3$ and uses equilateral prisms with $\tan 60^\circ = 1.73$. Lens structures are usually symmetric with respect to the optical axis, and thus the

effective aperture is simply two-fold the aperture of a half lens. For the one-dimensionally focusing clessidra the result according to Jark *et al.* (2004*b*) is then

$$A_{\rm geo} = 2\,J_{\rm max} h \tag{1}$$

and

$$\begin{aligned} A_{\rm eff} &= 2\sum_{j=1}^{J_{\rm max}} \int_0^h \exp\left(-\frac{2jM}{\mathrm{AL}\tan\varphi}\,y\right) \mathrm{d}y \\ &= \frac{\mathrm{AL}\tan\varphi}{M} \sum_{j=1}^{J_{\rm max}} \frac{1}{j}\left[1-\exp\left(-\frac{2Mh}{\mathrm{AL}\tan\varphi}\,j\right)\right]. \end{aligned} \tag{2}$$

Now, when a slit limits the accepted area in the focal plane, one has to modify the calculation for the effective aperture by limiting the integration to the active geometrical aperture, *i.e.* to the part of the geometrical aperture, $A_{\rm act}$, which will effectively refract the incident radiation into the slit (Jark, 2004). For the in-focus photon energy E_0 the active geometrical aperture is identical to the geometrical aperture and the smallest useful slit setting is the re-imaged source size. For photons of differing photon energy E the focal planes will be found at other distances and thus part of the refracted photons will hit the slit blades. Jark (2004) showed that they will have been refracted in the outer part of the geometrical lens aperture, which is then inactive for monochromatization purposes.

In the thin-lens approximation a plane wave is refracted to a focus when the refraction angle increases in the focusing object linearly with distance from the optical axis. This is also applicable for the prism array lenses. Now consider a lens with a focal length f at a source distance p from a source of size s. The exit-slit setting S in the image plane at a distance q from the lens may eventually be larger than the ideally re-imaged source according to

$$S = mi = ms(q/p) \qquad \text{with } (m \geq 1). \tag{3}$$

The focusing will be considered to be source size limited with a focus size much larger than the diffraction limit. From the study by Jark (2004), one can then readily derive the active geometrical aperture for off-focus photon energies, which remains symmetric with respect to the optical axis of the lens, as

$$\begin{aligned} A_{\rm act}(E > E_0) &= 2s\,\frac{f}{p}\,\frac{1}{1-(E_0/E)^2}\,\frac{m+1}{2}, \\ A_{\rm act}(E < E_0) &= 2s\,\frac{f}{p}\,\frac{1}{(E_0/E)^2-1}\,\frac{m+1}{2}. \end{aligned} \tag{4}$$

The corresponding maximum row index is given by

$$J_{\rm act,max} = A_{\rm act}/2h. \tag{5}$$

This active geometrical aperture for off-focus photon energies can be minimized by operating the lens with short focal length at a small source and with an exit slit, which is matched to the re-imaged source size, *i.e.* for $m = 1$. The active aperture for this case can be further reduced, when the central part of the lens is not contributing to the focused flux. For this purpose, Jark (2004) had proposed the introduction of a wire, which Liu *et al.* (2012) used in their experiment. Such an absorbing wire of diameter W on the optical axis and just downstream of the lens can easily be accommodated in the calculation as one will only have to substitute the lower index for the summation in (2) by $j = J_{\rm min} = W/2h$. It can be helpful for optimizations to consider that the effective aperture for this latter case can be obtained by subtracting the effective aperture corresponding to the wire from the effective aperture of the active aperture of the unobstructed lens.

In a prism array lens one will try to keep the prefactor in the argument of the exponential function in (2),

$$a = \frac{2Mh}{\mathrm{AL}\tan\varphi}, \tag{6}$$

as small as possible. For out-of-focus photon energies E the row index corresponding to the active aperture $J_{\rm act,max}$ according to (5) is rather small leading thus mostly to $aJ_{\rm act,max} < 1$. In this case one can substitute the summation in (2) by an integration and one can truncate the result at the third-order term. Then the effective aperture corresponding to the active aperture can be calculated as

$$\begin{aligned} A_{\rm act,eff}\left(J_{\rm act,max} > J_{\rm min}\right) = 2h\left(J_{\rm act,max} - J_{\rm min}\right) \\ \times\left[1-\frac{a}{4}\left(J_{\rm act,max}-J_{\rm min}\right)\right. \\ \left.+\frac{a^2}{18}\left(J_{\rm act,max}-J_{\rm min}\right)^2\right]. \end{aligned} \tag{7}$$

This latter expression cannot be applied in the vicinity of the in-focus photon energy when $J_{\rm act,max} \simeq J_{\rm max}$, in which case (2) has to be used. Obviously one has $A_{\rm act,eff}(J_{\rm act,max} \leq J_{\rm min}) = 0$. The optimization of the lens for small spectral resolution will then require the active geometrical aperture to be minimized according to (7) for off-focus photon energies by the appropriate choice of $J_{\rm min}$, while maximizing the effective aperture according to (2) for the in-focus photon energy.

3. Discussion of experimental data

In order to compare calculations based on (2) and (7) with the experimental data presented by Liu *et al.* (2012), one has to multiply the effective aperture with the emission characteristics of the storage ring and with the transmission of beamline components like filters. In the reported case an aluminium filter of thickness 0.25 mm protected the lens from the high heat load emitted at smaller and unused photon energies. The emitted photon flux was taken per constant energy interval. For this calculation the tabulated *h2y* function (X-ray Data Booklet, 2009) describing the on-axis photon flux density was accordingly modified for the experimental conditions, *i.e.* for a bending-magnet source with a critical energy of 6.25 keV as used by Liu *et al.* (2012). The calculations then refer to the expected transmitted photon flux per constant energy interval. They were made for the parameters of the lens as operated by Liu *et al.* (2012) without any absorbing wire and with different exit-slit settings. Liu *et al.* (2012) used $p = 12$ m, $f = 0.515$ m, $s = 0.2$ mm, $h = 12$ µm, $M = 8$, $\tan\varphi = 0.78$ and the SU8 resist. For

the latter the composition in terms of weight fractions is assumed to be C(0.727)O(0.182)H(0.069)Sb(0.014)F(0.006)-S(0.002) (Simon, 2010). The optical constants for this composition were obtained from the tabulated values of Henke *et al.* (1993), as was the transmission of the aluminium filter. The row index for in-focus operation was limited to J_{max} = 83, corresponding to the operated 2 mm aperture in front of the 2.9 mm-high centrally symmetric lens. The different pinholes in the focal plane with diameters of 20 µm, 30 µm, 50 µm and 100 µm were modelled with straight slits with apertures reduced by the ratio $\pi/4$. Then the slits correspond to approximately m = 1.6, m = 2.4, m = 4 and m = 8, respectively. The calculations were made for the in-focus photon energy E_0 = 15.7 keV, as chosen by Liu *et al.* (2012). They cover the reported spectral range of 7 keV to 22 keV, for which the behaviour is presented in Fig. 2. For comparison purposes the calculations are normalized at the in-focus photon energy of 15.7 keV with the exception of the simulation for the 16 µm slit, which was multiplied additionally by a factor of 1.6. This will make the calculations appear relative to each other similar to the experimental data as presented by Liu *et al.* (2012). The energy-dependent response function of the detection system for this experiment is unknown, so a direct comparison of the calculations with the experimental data is not possible. Nevertheless, the systematic relative variation depending on the slit size can be compared directly. For this aspect the relative intensities in the calculations for the off-focus tails are in very good agreement with the experimental data. This can be noted in particular from the curves for the slits measuring 16 µm and 40 µm, which almost fall onto each other on both sides of the maximum; after that the calculations for the 16 µm slit are increased by 60% with respect to the calculations for the 40 µm slit. In the experiment the same increase by 1.6 is applied to the corresponding data for the 20 µm pinhole compared with the 50 µm pinhole, and then the same coincidence is observed. One can note that the width of any peak at the half-maximum intensity is rather small and that the slopes at half intensity are rather steep and of almost equal amount. This allows us to compare the expected spectral resolution directly with the experimental data as reasonable detector response functions will not alter the calculated value appreciably. The available relative bandpass was found to decrease with decreasing slit size from about 10% to 4%. For the larger slits the halfwidth in the experimental data is found to differ by only 3–5% from the calculated values. Instead, for the smallest 16 µm slit the calculation predicts a 10% smaller spectral resolution. This agreement indicates a high-quality prism structure. A similar good agreement is found between the experiment and the calculations when central absorbing wires improve the relative spectral resolution to 2% by significantly reducing the tails at off-focus photon energies. Thus state-of-the-art prism array lenses can provide the performance which one would predict with the presented analytical approach for unobstructed prism arrays as well as for lenses operated with a central obstruction. Then the presented approach can be used for more systematic optimizations.

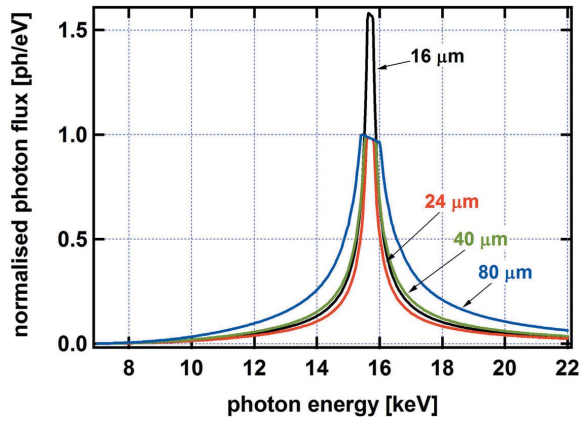

Figure 2
Simulations for the photon flux depending on photon energy to be expected at the exit slit behind a prism array with the parameters and the boundary conditions reported by Liu *et al.* (2012). From the bottom to the top the calculations are for a symmetric prism array lens and for exit slits measuring 24 (red line), 16 (black), 40 (green) and 80 µm (blue) as an approximation for 25% larger circular apertures with diameters of 30, 20, 50 and 100 µm, respectively. The maxima are made to coincide at the operation energy of 15.7 keV, with the exception of the calculation for the 16 µm slit which is put 60% higher. The latter modification was also made by Liu *et al.* (2012) in their presentation of experimental data.

4. Discussion of improved operation schemes

The formalism derived here can be applied to symmetric lenses as well as to half lenses. Obviously the second half in a symmetric lens will collect additional photon flux; however, it will not contribute to any improvement in the spectral resolution. Now consider an incident beam of limited vertical size, as will always be found in synchrotron radiation beamlines for harder X-rays (X-ray Data Booklet, 2009). Assume also that one will always want to reduce the tails at off-focus photon energies by use of an obstruction. Then it can be advantageous to use a half lens, provided that it can be made with the same geometrical aperture of the full lens with correspondingly increasing number for J_{max}. The latter aperture increase will thus provide improved spectral resolution. However, one has to accept some loss of transmitted flux compared with the symmetric lens, as the added area with large row index will provide a reduced efficiency. On the other hand, the transmitted bandpass and the spectral purity can now be adjusted simply by moving the corresponding low-index rows into the shadow of the beam-defining aperture in a vertical lens translation. So one no longer has to sacrifice incident flux in an eventually required central lens obstruction. The scheme for the lens operation in this way is shown in Fig. 3. It should be noted that the focus position will move in the vertical direction simultaneously with the lens translation. For a fixed lens position one can also adjust the spectral bandpass by varying the exit-slit size. In this way flux can be gained at the expense of reduced spectral purity.

4.1. Fixed focus tuning scheme

For a monochromator it would be highly desirable to keep the exit slit at a fixed position. This can be achieved in a prism array lens by rotating it around the yaw axis by the angle α.

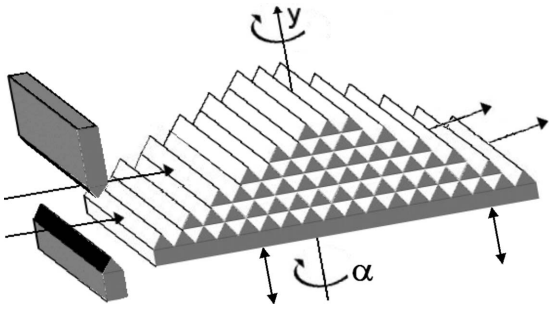

Figure 3
Scheme of a clessidra half-lens operated behind a beam-limiting aperture. The spectral resolution and the spectral purity behind this lens can be adjusted by translating it perpendicularly to the incident beam in the direction y (double-headed arrows). With sufficiently wide prisms the photon energy can be tuned in a stationary exit slit when the lens is rotated by the angle α around the vertical axis y.

Such an operation scheme has not been proposed yet for prism array or other kinoform lenses (Aristov *et al.*, 2000). Indeed, the limited depth to which these structures can be etched into material in processes utilizing lithographic techniques will not permit such an operation. This is clearly the case for the reported desktop monochromator with only 0.1 mm-wide prisms, which needs to be operated at $\alpha = 0^\circ$ (Liu *et al.*, 2012). On the other hand, Simon (2010), Simon *et al.* (2010) and Nillius *et al.* (2011) have already produced very wide prism array structures, which they wind up in order to fabricate rolled prism lenses that focus bi-dimensionally. Instead of being wound up, the thin foils could also be stacked to form a clessidra with very wide prisms, as is shown in Fig. 3. The increased prism width will then allow us to rotate the lens around an axis, which is perpendicular to the incident beam and to the prism bases. In such a lens the angle at the prism tip measured in the direction of the beam trajectory can then be varied. This will change the equation for the calculation of the focal length of the clessidra lens from $f = h\tan\varphi/2\delta M$ (Jark *et al.*, 2008; Liu *et al.*, 2012) to the more general expression

$$f = \frac{h\tan\varphi}{2\delta M}\cos\alpha. \qquad (8)$$

Here, δ is the refractive index decrement from unity for the lens material.

Then a fixed-focal-length operation can be realised for constant ratios $(\cos\alpha)/\delta$, and, as the refractive index decrement varies according to $\delta \propto \lambda^2 \propto E^{-2}$ (λ = photon wavelength) (James, 1967), the variation in the focused photon energy E is $E = E_0/(\cos\alpha)^{1/2}$, when E_0 is the in-focus photon energy for $\alpha = 0^\circ$. Note that in this tuning scheme the phase continuity in the transmitted wavefield can only be achieved for one particular combination of photon energy E, yaw angle α and prism base width, while for all other photon energies phase discontinuities will be observed in correspondence with the borders between different rows. This will not permit us to achieve diffraction-limited focusing, and the focus size will be limited at best to about the height of the prisms (Jark *et al.*, 2008).

Reasonable lens dimensions are maintained for $\alpha < 65^\circ$, which then provides tuning between E_0 and $1.5E_0$. If a beam width of b is proposed to be realised in a lens with a maximum extent in beam direction of L for $\alpha = 0^\circ$, then the prism width B needs to be $B = L\tan\alpha + (b/\cos\alpha)$. For an example lens with $L = 10$ mm and $\alpha_{\max} = 65^\circ$ one obtains $B = 33.3$ mm, when one would like to operate with a $b = 5$ mm-wide monochromated line. The beam trajectory in the prism bases of the last prism row with touching prisms measures then at most 23.66 mm. Now in the last row with index $J_{\max} = 83$, which Liu *et al.* (2012) illuminated in their lens, the beam trajectory in the prism bases measured $L_{\rm traj} = 20.6$ mm. This was more than three-fold the attenuation length of the lens material of 6.3 mm (Henke *et al.*, 1993) for the in-focus photon energy of 15.7 keV. If now the ratio 3 is taken as a practical limit for efficiently functioning prisms arrays then the tuning in the example lens could be started at a photon energy of 12.5 keV, where the attenuation length in SU8 is 3.4 mm. At the upper tuning limit of 18.7 keV for $\alpha_{\max} = 65^\circ$, the attenuation length is increasing to 10 mm. With a smaller ratio than 3 at this point the lens should work more efficiently. Likewise it will work more efficiently towards larger photon energy with accordingly increased lower tuning limit. For wide-bandpass operation in the indicated photon energy range 12.5–18.7 keV, Liu *et al.* (2012) needed to move the exit slit behind a stationary lens by 0.4 m from 0.325 m up to 0.725 m from the lens. At this point one still needs to recognize that the rotation in yaw will also produce a lateral refraction at any prism interface. Unlike in the dispersion direction, the lateral refraction will not lead to an angular deviation in the beam trajectory but only to a lateral beam displacement in the passage through any prism. The latter displacement increases with increasing path length in material up to $[\delta/\tan(90^\circ - \alpha)]L_{\rm traj}$. Consequently the lateral refraction will introduce aberrations. However, for the indicated limited rotation in yaw they will produce a beam broadening, which remains significantly below 1 µm. Consequently this defect can be ignored in almost all practical monochromator concepts.

By use of this new monochromator scheme a relative spectral resolution of the order of 2% is always feasible in slits which are larger than the prism height, when the low-index rows do not participate in the focusing.

5. Conclusion

It is shown that the bandpass behind prism array lenses can easily be predicted analytically for full aperture lenses and for lenses operated with a central obstruction. State-of-the-art lenses were found to provide the expected performance. It is proposed that half-lenses can be operated more flexibly as wide-bandpass monochromators as the central obstruction is then not needed and the undesired low-index rows of a lens can be excluded more easily from the monochromatization by use of an aperture. A solution for the inconvenient significant variation in the focal distance with photon energy behind a stationary prism array lens is identified. The focus can be kept in a fixed focal plane when the lens is rotated in yaw.

References

Aristov, V., Grigoriev, M., Kuznetsov, S., Shabelnikov, L., Yunkin, V., Weitkamp, T., Rau, C., Snigireva, I., Snigirev, A., Hoffmann, M. & Voges, E. (2000). *Appl. Phys. Lett.* **77**, 4058–4060.

Cederström, B. (2001). PhD thesis, Royal Institute of Technology, Stockholm, Sweden (http://www.dissertations.se/about/Björn+Cederström/).

Fredenberg, E., Cederström, B., Aslund, M., Ribbing, C. & Danielsson, M. (2008). *X-ray Opt. Instrum.* **2008**, 635024.

Fredenberg, E., Cederström, B., Nillius, P., Ribbing, C., Karlsson, S. & Danielsson, M. (2009). *Opt. Express*, **17**, 11388–11398.

Henke, B. L., Gullickson, E. M. & Davis, J. C. (1993). *Atom. Data Nucl. Data Tables*, **54**, 181–342 (http://www-cxro.lbl.gov/optical_constants/).

James, R. W. (1967). *The Optical Principles of the Diffraction of X-rays.* Ithaca: Cornell University Press.

Jark, W. (2004). *X-ray Spectrom.* **33**, 455–461.

Jark, W., Pérennès, F., Matteucci, M. & De Caro, L. (2008). *Modern Developments in X-ray and Neutron Optics, Springer Series in Optical Sciences*, Vol. 137. Berlin: Springer.

Jark, W., Pérennès, F., Matteucci, M., Mancini, L., Montanari, F., Rigon, L., Tromba, G., Somogyi, A., Tucoulou, R. & Bohic, S. (2004*b*). *J. Synchrotron Rad.* **11**, 248–253.

Lengeler, B., Schroer, C., Tümmler, J., Benner, B., Richwin, M., Snigirev, A., Snigireva, I. & Drakopoulos, M. (1999). *J. Synchrotron Rad.* **6**, 1153–1167.

Liu, T., Simon, R., Batchelor, D., Nazmov, V. & Hagelstein, M. (2012). *J. Synchrotron Rad.* **19**, 191–197.

Nillius, P., Karlsson, S., Cederström, B., Fredenberg, E. & Danielsson, M. (2011). *Opt. Lett.* **36**, 555–557.

Simon, M. (2010). PhD thesis, Karlsruher Institut für Technologie, Karlsruhe, Germany.

Simon, M., Reznikova, E., Nazmov, V., Grund, T. & Last, A. (2010). *AIP Conf. Proc.* **1221**, 85–90.

Vaughan, G. B. M., Wright, J. P., Bytchkov, A., Rossat, M., Gleyzolle, H., Snigireva, I. & Snigirev, A. (2011). *J. Synchrotron Rad.* **18**, 125–133.

X-ray Data Booklet (2009). *X-ray Data Booklet*, §2.1. Center for X-ray Optics and Advanced Light Source, Lawrence Berkeley National Laboratory, Berkeley,CA, USA (http://xdb.lbl.gov/xdb-new. pdf; http://xdb.lbl.gov/Section2/Sec_2-1.html).